

# Mechanical properties of ultrahigh molecular weight polyethylene–polypropylene blend films produced by gelation/crystallization from solution

Chie Sawatari and Suzuko Satoh

Faculty of Education, Shizuoka University, Ohya 422, Japan

and Masaru Matsuo\*

Department of Clothing Science, Faculty of Home Economics, Nara Women's University, Nara 630, Japan

(Received 7 September 1989; accepted 8 November 1989)

Films of a polyethylene–polypropylene blend were prepared by gelation/crystallization from semidilute solutions using ultrahigh molecular weight polyethylene ( $M_v = 6 \times 10^6$ ) and polypropylene ( $M_v = 4.4 \times 10^6$ ). The polyethylene/polypropylene (PE/PP) compositions chosen were 75/25, 50/50 and 25/75. The elongation was carried out in a hot poly(ethylene glycol) oil bath at 140°C. The mechanical properties of the resultant gel films were dependent upon the PE/PP compositions at each draw ratio. This interesting phenomenon is discussed using the second-order orientation factors of the *c* axes of polyethylene and polypropylene within the blend films. It turns out that the orientation factors of the polyethylene and polypropylene phases within the blend films at each draw ratio are different from those of their individual homopolymers with the corresponding draw ratio and this tendency is pronounced for blend films with a draw ratio of 20. Therefore, it is insufficient to explain the dependence of PE/PP composition on the storage and loss moduli by a composite law based on a simple model system in which polyethylene layers lie adjacent to polypropylene layers with the interfaces parallel and perpendicular to the stretching direction and the morphological properties of the two phases within the blend films are equivalent to those of their individual homopolymers at each draw ratio.

(Keywords: polyethylene–polypropylene blend; PE/PP compositions; gel films; orientation factor)

## INTRODUCTION

The crystal lattice moduli of polyethylene and isotactic polypropylene have been measured by X-ray diffraction using ultradrawn films which were produced by gelation/crystallization from dilute solutions<sup>1,2</sup>. The measured crystal lattice modulus of polyethylene was in the range 213–229 GPa<sup>1</sup> and that of polypropylene was 39–43 GPa<sup>2</sup>. The maximum Young's moduli of polyethylene and polypropylene approach 216<sup>2</sup> and 40.4 GPa<sup>3</sup>, respectively. The considerable difference in the crystal lattice moduli between polyethylene and polypropylene is due to the fact that the polyethylene chain has a fully extended (all *trans*) planar zigzag conformation, while the isotactic polypropylene has *trans* and *gauche* conformations. In spite of the excellent mechanical properties of polyethylene, its thermal properties are poorer than those of polypropylene. The apparent melting points of ultradrawn polyethylene and polypropylene films measured by differential scanning calorimetry were  $\approx 155^4$  and  $\approx 178^{\circ}\text{C}^3$ , respectively.

To produce films with improved mechanical and thermal properties, ultradrawing of blend gel films of polyethylene and polypropylene has been studied in

terms of morphological aspects in previous work<sup>5</sup>. Films of polyethylene and polypropylene blend were prepared by gelation/crystallization from semidilute solutions by using ultrahigh molecular weight polyethylene (UHMWPE) ( $M_v = 6 \times 10^6$ ) and ultrahigh molecular weight polypropylene (UHMWPP) ( $M_v = 4.4 \times 10^6$ ) according to the method of Smith and Lemstra<sup>6–8</sup>. The polyethylene–polypropylene (PE/PP) compositions were 75/25, 50/50 and 25/75. The maximum drawability was affected by composition. This interesting phenomenon was discussed in terms of wide-angle X-ray diffraction (WAXD), small-angle light scattering (SALS), optical microscopy and scanning electron microscopy (SEM). Through a series of experimental results, it turned out that the facile drawability of the blend gel films with draw ratios  $> 50$  is due to the existence of a suitable level of entanglement mesh between the polyethylene and polypropylene chains in spite of their incompatibility in solution.

In the present work, our focus is on the mechanical properties of ultradrawn blend gel films. The characteristic mechanical properties of the blend films are discussed in terms of their morphological properties and they are also analysed in relation to the mechanical properties of their individual homopolymers by using a model system where polyethylene phase is attached to the polypropylene phase as discussed below.

\* To whom correspondence should be addressed

## EXPERIMENTAL SECTION

The samples used in this experiment were linear polyethylene and polypropylene with molecular weights of  $6 \times 10^6$  and  $4.4 \times 10^6$ , respectively, as in previous work<sup>5</sup>. The solvent was decalin. The gel films were prepared according to the methods described previously<sup>5</sup>. Strips of the gel film were clamped in a manual stretching device and were placed in a poly(ethylene glycol) (PEG) bath at 140°C and immediately elongated to the desired draw ratio. After the samples had been stretched, the stretcher with the samples was annealed at 140°C for 2 h and quenched to room temperature. The stretcher and the sample were immersed in a hot water bath at 80°C for several minutes to remove PEG. The drawn films were immersed in ethanol for 1 week and vacuum dried to remove residual traces of antioxidant di-*t*-butyl-*p*-cresol and PEG completely.

The complex dynamic tensile modulus functions were measured at a frequency of 10 Hz over the temperature ranges  $-150$  (or  $-100$ )–190°C by using a viscoelastic spectrometer (VES-F) obtained from Iwamoto Machine Co. Ltd. The length of the specimen between the jaws was  $\approx 40$  mm. During measurements, the film was subjected to a static tensile strain to place the sample in tension during the axial sinusoidal oscillation which had a peak deformation of 0.05%. The complex dynamic modulus was measured by imposing a small dynamic strain to assure linear viscoelastic behaviour of the specimen. Before the measurements were made, the undrawn films were annealed for 1 h at 90°C and the drawn specimens were annealed for 1 h at 120°C.

Young's modulus and tensile modulus were measured by using an Instron type test machine at a slow speed of  $2 \text{ mm min}^{-1}$ ; the sample length between the jaws was 40 mm.

The X-ray diffraction measurements were made by a 12 kW rotating anode X-ray generator (RDA-rA) with  $\text{CuK}_\alpha$  radiation. X-ray diffraction intensity distribution was measured for three crystal planes, the (110), (040) and ( $\bar{1}$ 13) planes, of polypropylene and for the (002) plane of polyethylene with an ordinary horizontal scanning type goniometer operating at a fixed time step scan of  $0.1^\circ$  interval over twice the Bragg angle  $2\theta_B$  from  $11$  to  $19^\circ$  and from  $39$  to  $46^\circ$  for polypropylene and from  $71$  to  $77^\circ$  for polyethylene. The horizontal scanning was done at fixed angles by rotating the specimen stepwise about the film thickness direction at  $5^\circ$  intervals. After applying corrections to the observed X-ray diffraction intensity (for air scattering, background noise, polarization and absorption) and subtracting the contribution of the amorphous halo from the corrected total intensity curve, the intensity is believed to be due to the diffraction from crystalline phase. The intensity is separated into the contribution from the individual crystal planes. As for the (110) and (040) planes of polypropylene, the contribution from the (130) plane of polypropylene and the (110) plane of polyethylene must be considered. The separation was done on the basis of the assumption that each peak has a symmetric form given by a Lorentz function. The detailed treatment has already been described elsewhere<sup>9,10</sup>.

Small angle light scattering (SALS) patterns were obtained with a 15 mW He-Ne gas laser as a light source. Diffuse scattering was avoided by sandwiching the specimen between cover glasses with silicon oil as an immersion fluid.

The density of the films was measured by pycnometry with chlorobenzene-toluene as the medium. Since the density was very dependent on the presence of residual antioxidant and PEG in the films, great care was taken to remove them. For this reason, the drawn specimen was cut into fragments and immersed in ethanol for 30 d and subsequently vacuum-dried for 1 d before the density was measured.

Birefringence was measured by an optical microscope with crossed polaroids, using a Berek compensator for measuring the retardation.

## RESULTS AND DISCUSSION

Figure 1 shows Young's modulus of the blend gel films with the indicated draw ratios measured at 20°C. Young's modulus of the specimen decreases with increasing polypropylene content except for the specimen with  $\lambda = 20$ , whose Young's modulus increases with increasing polypropylene content. The result at  $\lambda = 20$  contradicts the general concept of polymer science, since the crystal lattice modulus in the chain direction of polyethylene (213–229 GPa)<sup>1</sup> is much higher than that of polypropylene (41–43 GPa)<sup>3</sup>. This interesting mechanical property is also observed for the corresponding tensile strength shown in Figure 2: tensile strength increases with increasing polyethylene content except for  $\lambda = 20$ , where tensile strength increases with increasing polypropylene content, although the tensile strength of polypropylene homopolymer is lower than the tensile strengths of the 50/50 and 25/75 blend films. This discrepancy is thought to be due to the morphological difference between the blend and the individual homopolymers. Incidentally, the values of Young's modulus and tensile strength of polypropylene film at  $\lambda = 100$  are lower than those reported previously<sup>3</sup>. This is probably due to the drawing condition; the drawing of this experiment was in PEG at 140°C and the drawing of the previous experiment was in a hot oven. It is believable that PEG molecules act as plasticizer.

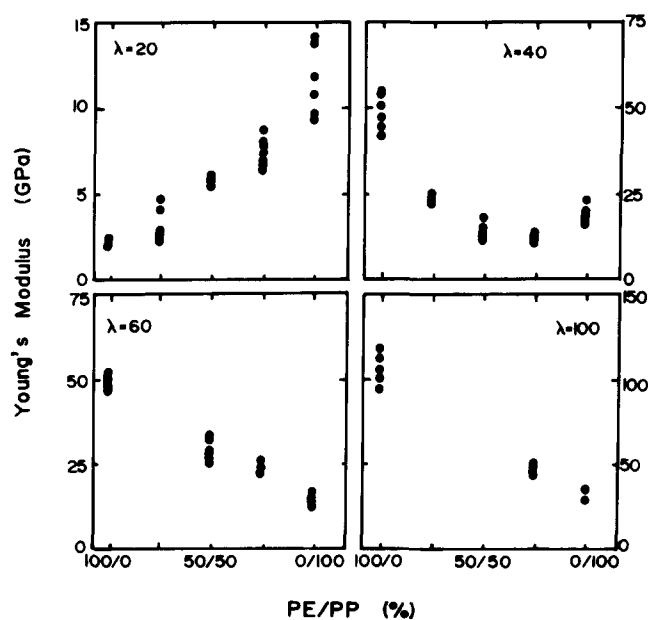


Figure 1 Young's modulus of the specimens for the PE/PP compositions indicated at various draw ratios

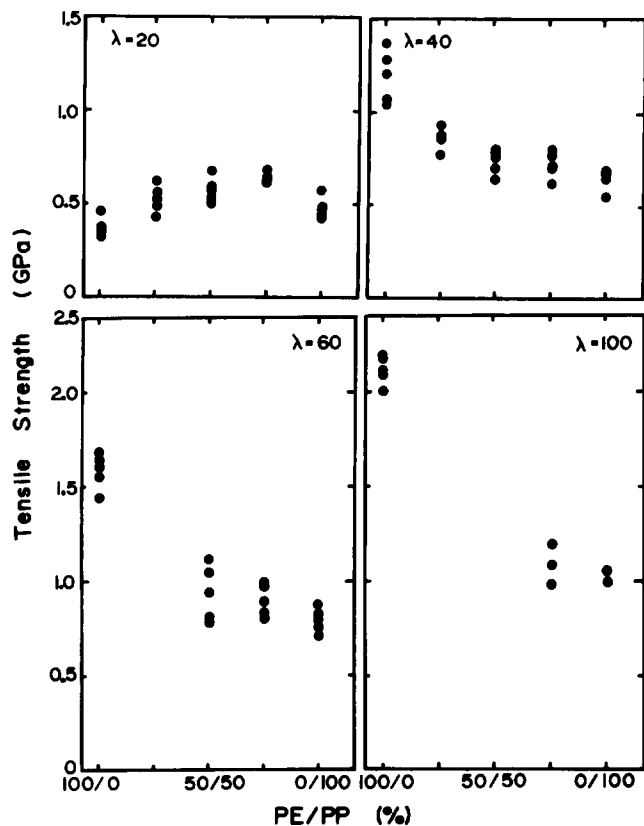


Figure 2 Tensile strength of the specimens for the PE/PP compositions indicated at various draw ratios

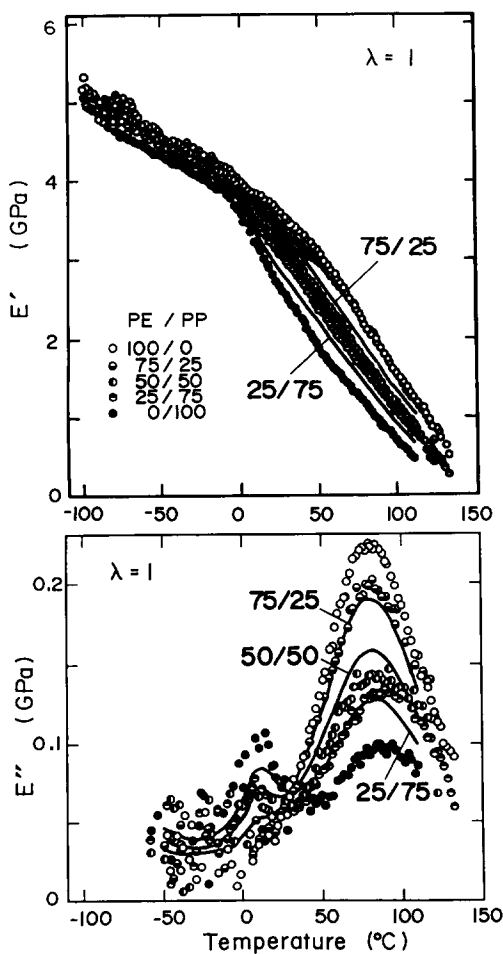


Figure 3 Temperature dependence of storage and loss moduli for undrawn gel films for the PE/PP compositions indicated: symbols, experimental results; —, theoretical results calculated on the basis of the model in Figure 14

To check these mechanical properties of the blend gel films, the complex dynamic tensile modulus was measured over a wide temperature range. All the plots (not the solid curves) in Figures 3–7 show the temperature dependence of storage and loss moduli at a frequency of 10 Hz for the undrawn and drawn gel films. In Figure 3, the storage modulus over the given temperature range increases with increasing polyethylene content. The storage modulus decreases with increasing temperature for all the specimens. This tendency is similar to the results observed by several authors for semicrystalline polymers. For the loss modulus, the  $\alpha$  transition around 80°C can be observed for all the specimens and the peak intensity becomes sharper with increasing polyethylene content. The  $\beta$  transition peak appearing in the temperature range -10–10°C decreases in intensity with increasing polyethylene content. The temperature dependence of the loss modulus for the  $\alpha$  transition of polyethylene is affected by crystallinity. The  $\alpha$  transition of polyethylene has been classified into two mechanisms, the  $\alpha_1$  and  $\alpha_2$ <sup>11–15</sup>. The  $\alpha_1$  mechanism is associated with grain boundary phenomena of deformation and/or rotation of crystallites (crystal mosaic block) within a viscous medium and the  $\alpha_2$  mechanism involves the crystal disordering transition due to the onset of torsional oscillation of polymer chains within the crystal lattice. The  $\beta$  transition is assigned to interlamellar grain boundary phenomena associated with orientational and distortional dispersions of amorphous phases between

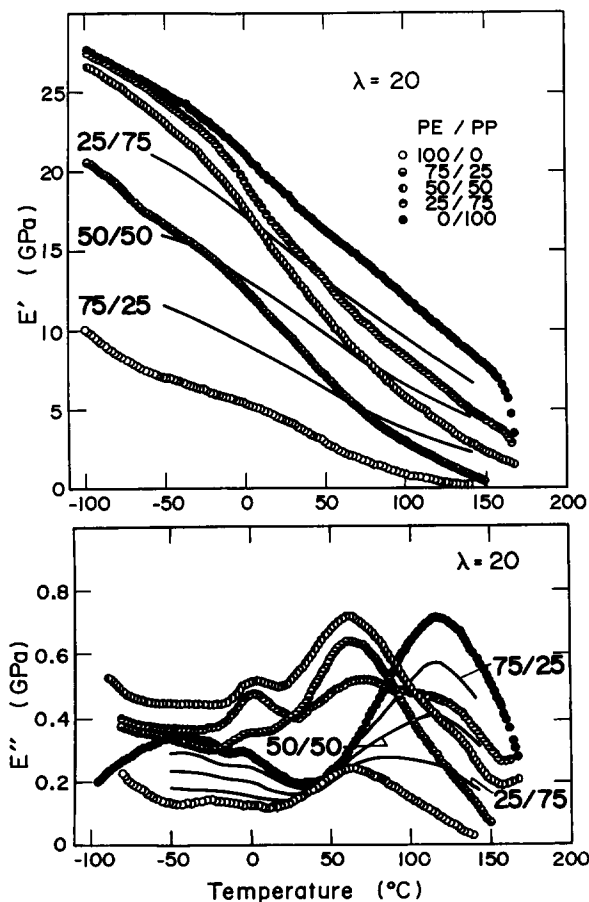
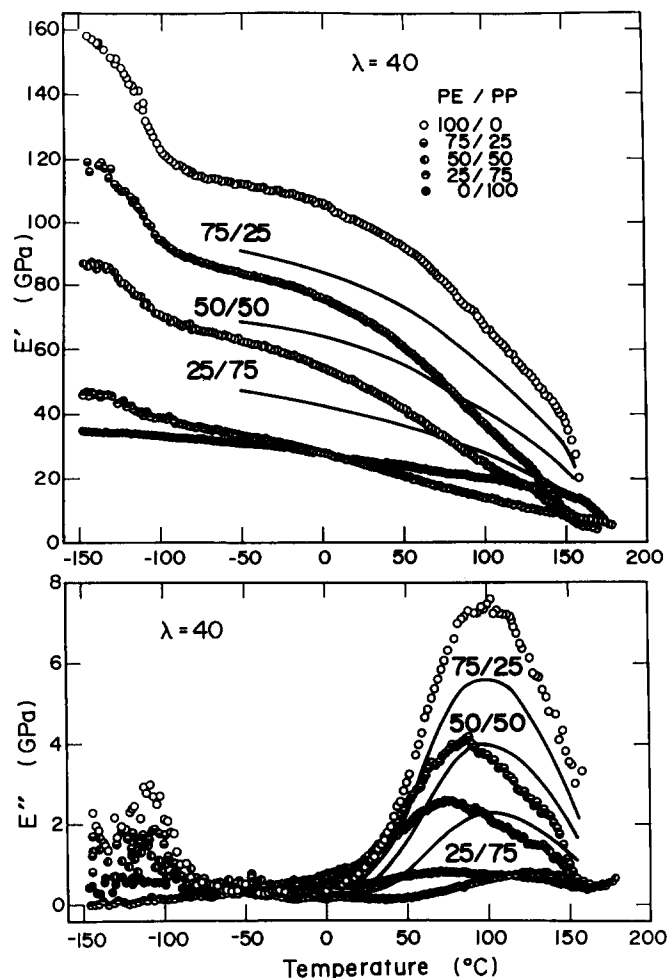


Figure 4 Temperature dependence of storage and loss moduli for drawn gel films ( $\lambda = 20$ ) for the PE/PP compositions indicated: symbols, experimental results; —, theoretical results calculated on the basis of the model in Figure 14



**Figure 5** Temperature dependence of storage and loss moduli for drawn gel films ( $\lambda=40$ ) for the PE/PP compositions indicated: symbols, experimental results; —, theoretical results calculated on the basis of the model in Figure 14

orienting lamellae<sup>14</sup>. The  $\beta$  transition of polyethylene cannot be observed for dried gel films because of high crystallinity,  $\approx 84\%$ <sup>15</sup>, but it could be observed for melt films whose crystallinities were  $< 60\%$ <sup>3</sup>. Accordingly, the  $\beta$  transition of the blend films in this experiment is evidently associated with the amorphous transition of polypropylene.

From the storage moduli curves in Figures 4–7, it is seen that the values for the specimen with  $\lambda=20$  decrease over the given temperature range with increasing polyethylene content, while those for the specimens with  $\lambda=40, 60$  and  $100$  increase with increasing polyethylene content. This satisfies the results of Figures 1 and 2. For the loss modulus, the peak position of the  $\alpha$  transition for the polyethylene homopolymer with  $\lambda=20$  appears around  $60^\circ\text{C}$ . With elongation, the  $\alpha$  transition peak shifts from about  $80^\circ\text{C}$  to lower temperature for the undrawn blend and polyethylene homopolymer, as shown in Figure 3, indicating imperfection of crystallites in the transformation process from a folded to a fibrous type. With further increase in draw ratio beyond 40, the  $\alpha$  peak shifts to higher temperature through the increase in perfection of crystallites, and the peak of the  $\beta$  transition disappeared owing to an increase in crystallinity of the polypropylene phase. The crystallinities were 76, 79 and 82% for the polypropylene homopolymer with  $\lambda=40, 60$  and  $100$ , respectively. These values were slightly

lower than those for polypropylene gel films with the corresponding draw ratios stretched in a hot oven under nitrogen<sup>3</sup>.

Note here that the storage moduli of the 25/75 blend films are lower than those of polypropylene homopolymers in the temperature range beyond  $0^\circ\text{C}$  for the specimen with  $\lambda=40$  and beyond  $120^\circ\text{C}$  for the specimens with  $\lambda=60$  and  $100$ . This is due to the fact that the orientational degree of the  $c$ -axes within the 25/75 blend film is lower than that within the polyethylene homopolymer at each draw ratio, and the mobility of the polyethylene chain within the blend film becomes greater with temperature. This analysis will be discussed later.

Returning to Figures 1 and 4, the question must be resolved why Young's modulus at room temperature and the storage modulus over the given temperature range decrease with increasing polyethylene content for the specimen with  $\lambda=20$ . To understand this behaviour, the orientation of the  $c$ -axes of polyethylene and polypropylene crystallites was estimated in terms of the second-order orientation factor. The second-order orientation factors  $F_{200}=0, -1/2$  and  $1$  correspond to random, perpendicular and parallel to the stretching direction, respectively. The orientation factor of polyethylene was obtained directly from the (002) plane, while that of polypropylene was calculated using the orientation factors of the (110), (040) and ( $\bar{1}13$ ) planes by Wilchinsky's equation<sup>16</sup>. They are shown in Figures 8 and 9. As can be seen in Figure 8, the orientation factor of polyethylene is affected by the PE/PP composition. The factor of the

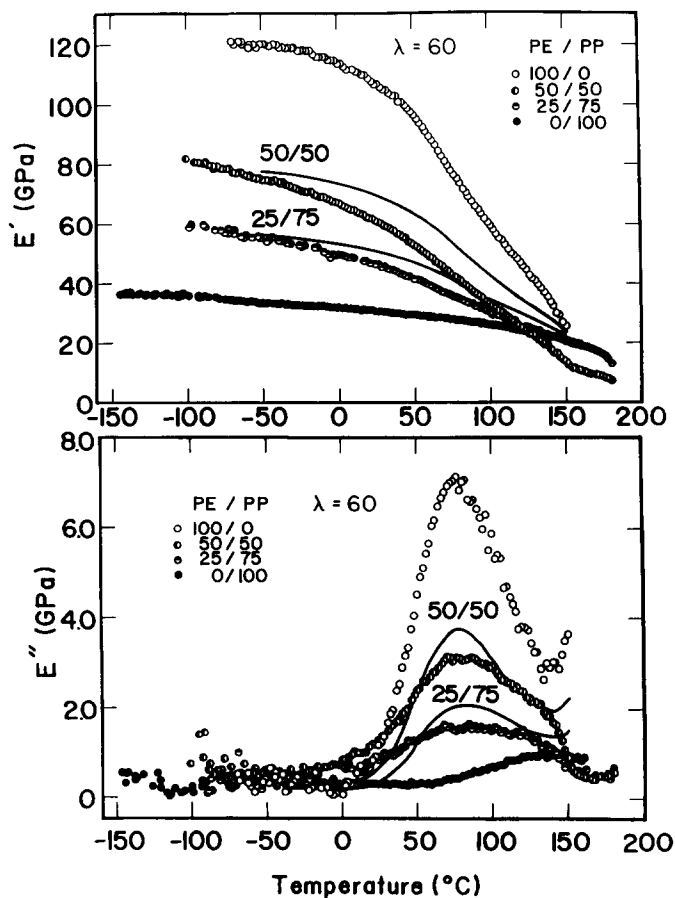


**Figure 6** Temperature dependence of storage and loss moduli for drawn gel films ( $\lambda=60$ ) for the PE/PP compositions indicated: symbols, experimental results; —, theoretical results calculated on the basis of the model in Figure 14

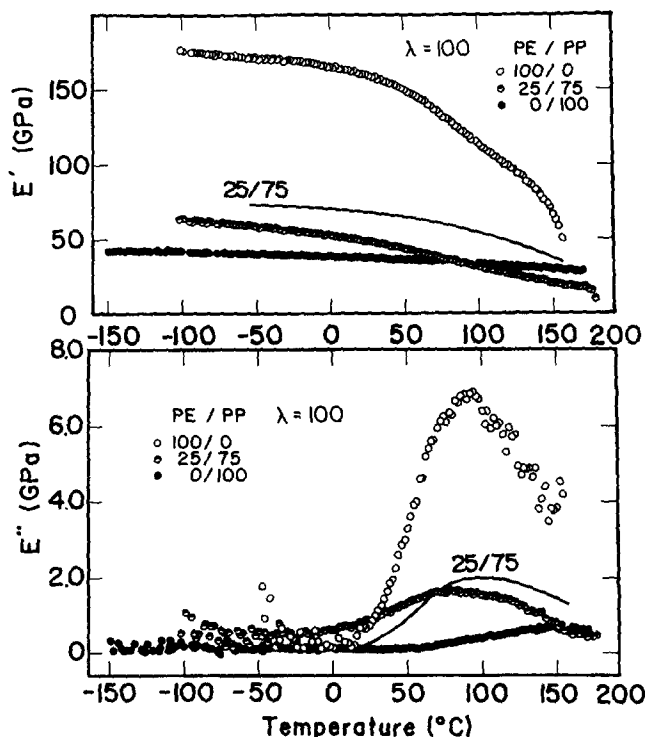


Figure 7 Temperature dependence of storage and loss moduli for drawn gel films ( $\lambda=100$ ) for the PE/PP compositions indicated: symbols, experimental results; —, theoretical results calculated on the basis of the model in Figure 14

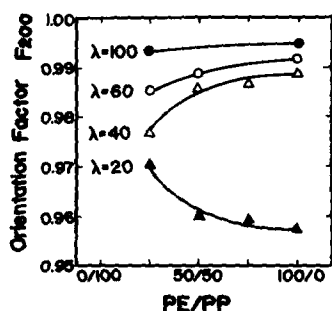


Figure 8 The second-order orientation factor of the *c*-axis of polyethylene phase within the gel films for PE/PP compositions indicated at various draw ratios

blend films with  $\lambda=20$  decreases with increasing polyethylene content, while the factors of the other blend films with draw ratios  $\geq 40$  increase. This indicates that the orientation of the *c*-axes within the blend films with  $\lambda=20$  is unusual. In contrast, the orientation factor of polypropylene crystallites of the specimens with  $\lambda=20$  decreases drastically with increasing polyethylene content, as shown in Figure 9. This tendency becomes less pronounced with increasing draw ratio but, beyond  $\lambda=60$ , the orientation factor is independent of PE/PP composition. The results in Figures 8 and 9 indicate that the unusual relationship between Young's (or storage) modulus and PE/PP composition for the specimens with  $\lambda=20$  is due to the fact that the orientational degrees of the *c*-axes of polyethylene and polypropylene crystallites decrease with increasing polyethylene content.

Figure 10 shows the nominal stress-strain relationship at  $\lambda=1, 20$  and 40 of the blend films and their homopolymers at a constant strain rate of  $2 \text{ mm min}^{-1}$  at  $140^\circ\text{C}$ . The curve profile is strongly affected by PE/PP composition. The curve for undrawn polypropylene film

exhibits a yield point at an initial draw ratio after which the stress decreases to  $\approx 20\%$  strain. The stress remains constant with further elongation. When the applied stress exceeds the yield stress, necking suddenly appears at a localized region in the specimen and subsequently grows continuously until the whole specimen is covered. In such a non-uniform drawing process, the decrease in transverse specimen dimensions with increasing length occurred mainly in the direction of the film thickness and much less in the film width, as has been observed for polyethylene gel film drawn at room temperature<sup>17</sup>.

As for the blend films, the yield point becomes more indistinct with increasing polyethylene content and the draw ratio corresponding to their yield point becomes higher. Finally, the yield point of the polyethylene homopolymer can be diminished and the nominal stress increases with draw ratio. This indicates that a surprising mobility of polyethylene chains within crystal lamellae occurred at  $140^\circ\text{C}$  close to the melting point of undrawn polyethylene gel film<sup>4</sup>. In this case, the crystal lamellae can readily be destroyed by elongation and do not act as rigid bodies.

The profile of the curves for the drawn film with  $\lambda=20$  is dependent on PE/PP composition. The curve of the polyethylene homopolymer exhibits a yield point at 8% strain after which the stress decreases until  $\approx 15\%$ . The stress increases with further elongation up to 80% and after then it levels off to 120% close to the breaking point. The drawing mode is non-uniform, similar to the behaviour of undrawn polypropylene films. This indicates that the polyethylene gel film with  $\lambda=20$  still remains crystal lamellae. The curve of the polypropylene gel film exhibits an indistinct yield point, after which the stress levels off until about 40% strain. The stress decreases gradually with further elongation. Such a decrease has

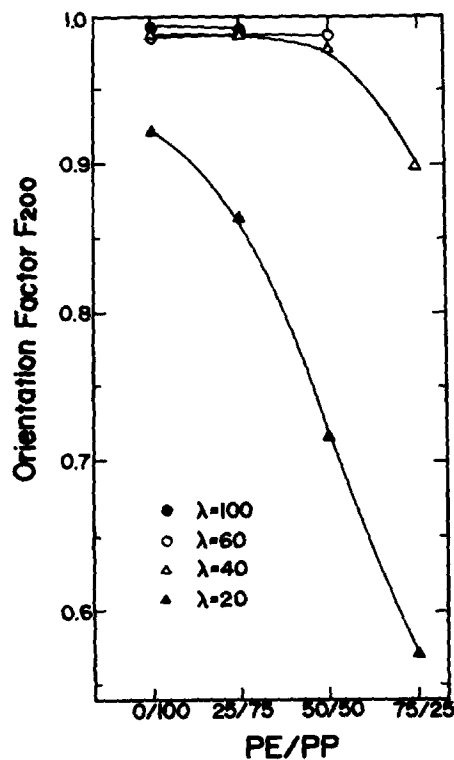


Figure 9 The second-order orientation factor of the *c*-axis of polypropylene phase within the gel films for PE/PP compositions indicated at various draw ratios

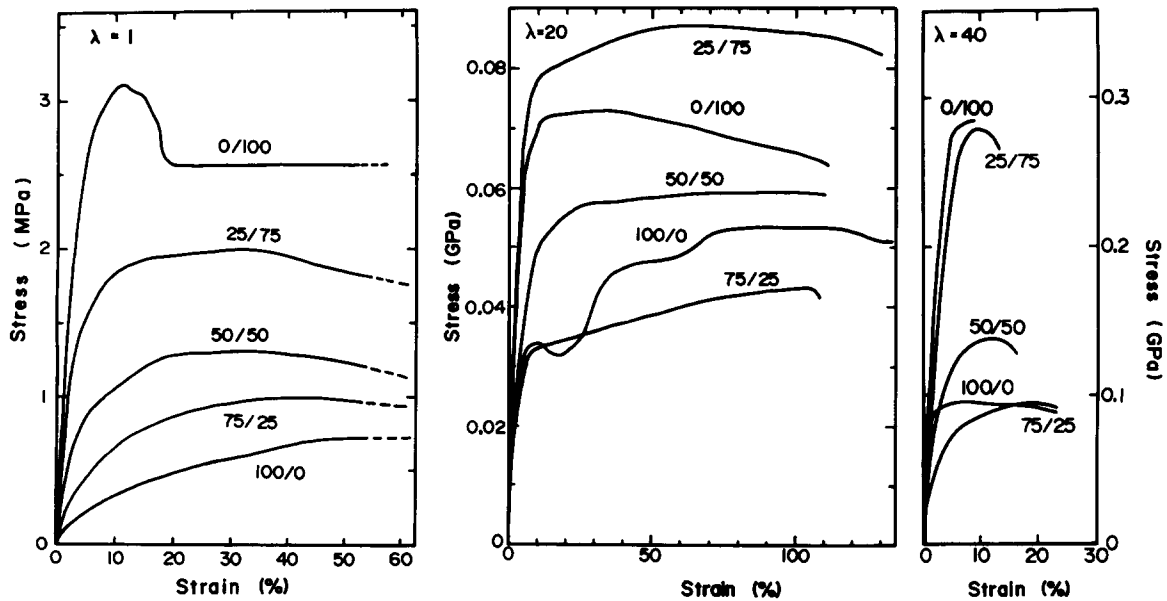


Figure 10 Stress-strain relationship for undrawn and drawn films for the PE/PP compositions indicated measured at 140°C

been observed when polymeric materials with high molecular orientation are drawn at a slow strain speed such as  $2\text{ mm min}^{-1}$  at room temperature. This is probably attributed to stress-relaxation under elongation due to the slippage of molecular chains. The stresses of the blend films with the 75/25 and 50/50 compositions increase until their breaking points with further elongation beyond their yield points. The question arises why the yield stress and Young's modulus of the 25/75 blend film are the highest in spite of the lowest content of polyethylene, whose crystal lattice modulus is higher than that of polypropylene. This is thought to be due to the fact that the orientational degree of the polyethylene crystal fibre axis (the *c*-axis) within the 25/75 blend is the highest among the three kinds of blend film, as shown in Figures 8 and 9.

For the films with  $\lambda = 40$ , stress increases with increasing polypropylene content except for the 75/25 blend. The tendency is quite different from the PE/PP composition dependence of Young's modulus and tensile strength at 20°C shown in Figure 2b. Such curve profiles of all the specimens indicate that measurements of tensile strength at 140°C are significant enough to postulate the existence of folded type crystals of polyethylene even at a draw ratio of 40 as well as the transformation of polypropylene crystallite from a folded to a fibrous type.

Figures 11 and 12 show the temperature dependence of birefringence measured for the gel films with the indicated PE/PP compositions at  $\lambda = 20$  and 40, respectively. The measurements were made for the specimens with a fixed dimension in the stretching direction. Because of an intrinsic birefringence value of polyethylene higher than that of polypropylene<sup>18,19</sup>, the birefringence of the blend films increases with increasing polyethylene content but the values are hardly affected by temperature up to 160°C higher than the apparent melting point (155°C) due to the superheating effect<sup>4</sup>. At temperatures beyond 160°C, however, the temperature dependences of birefringences of the blend films with  $\lambda = 20$  and 40 show different behaviour: drastic decreases in birefringence are observed for blend films with  $\lambda = 20$ . Judging from the birefringence behaviour in Figures 11 and 12, it may be

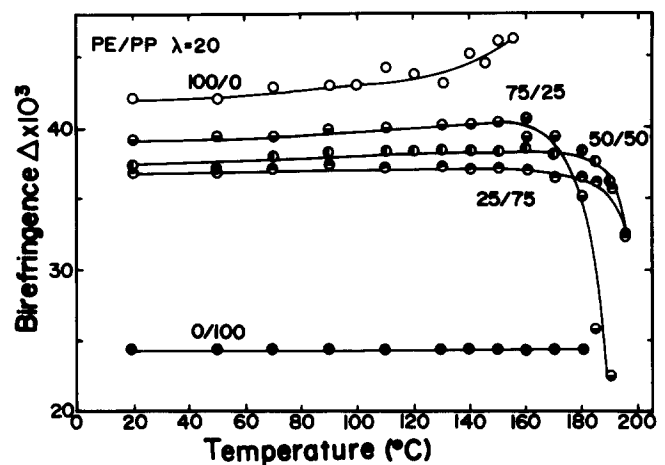


Figure 11 Temperature dependence of birefringence for specimens with the PE/PP compositions indicated at  $\lambda = 20$

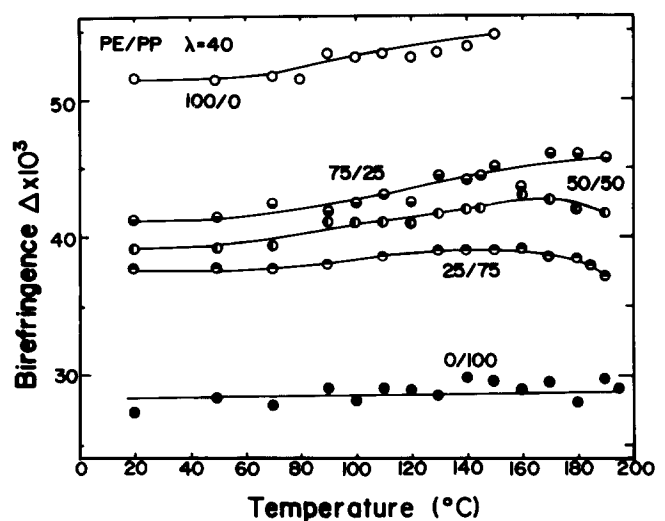


Figure 12 Temperature dependence of birefringence for specimens with the PE/PP compositions indicated at  $\lambda = 40$

expected that, around 160°C, oriented polyethylene crystallites within the blend films with  $\lambda=20$  are not free to allow a random orientation in the melt state because of the existence of entanglement mesh between polyethylene and polypropylene chains, but at temperatures beyond 160°C the mobility of polyethylene becomes active enough to increase orientational fluctuation due to stress relaxation. In contrast, with the fixed dimension, the very highly extended polyethylene chains within the blend films with  $\lambda=40$  are not free to allow an increase in orientational fluctuation even at temperatures beyond 160°C, because of the very dense arrangement of molecular chains, so that there exists no space to invoke the chain mobility within the specimen. This result also supports the previous results of WAXD patterns, which did not show diffraction rings but showed equatorial refractions of the (110) and (200) planes within the 25/75 blend film at  $\lambda=60$ , indicating that the *c*-axes of polyethylene are highly oriented with respect to the stretching direction<sup>5</sup>.

Figure 13 shows the SALS patterns under  $H_v$  polarization conditions as a function of temperature, measured for the 25/75 blend films with  $\lambda=20$  and 40. The pattern from the film with  $\lambda=20$  shows a diffuse X-type whose lobes are slightly extended in the vertical direction. Such a pattern characterizes scattering from rodlike textures

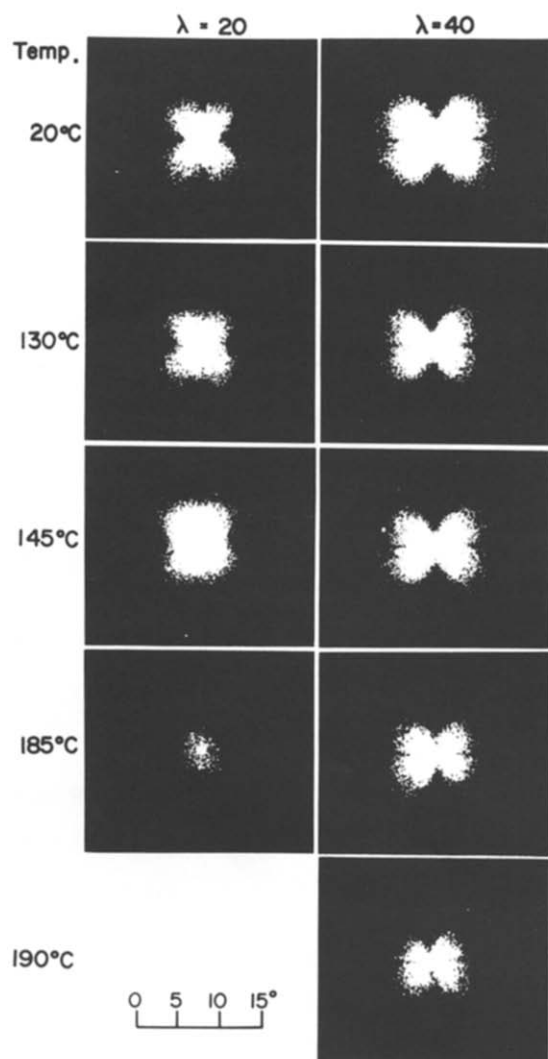


Figure 13 SALS patterns under  $H_v$  polarization condition as a function of temperature, observed for the 25/75 blend films with  $\lambda=20$  and 40

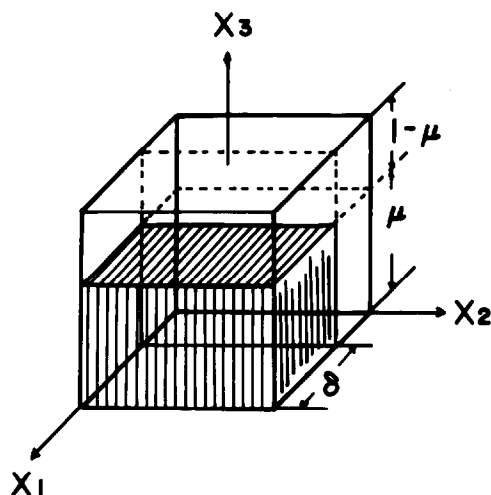


Figure 14 Composite structural unit of the blend system, in which the polyethylene phase is attached to both the  $X_3$  and the  $X_1$  faces of the polypropylene phase

under oriented crystallization<sup>20,21</sup>. With increasing temperature, the pattern becomes more indistinct and, at 185°C, the scattering shows an indistinct circular pattern. Thus it turns out that the active mobility of polymer chains is more pronounced with increasing temperature in spite of the fixed dimension in the stretching direction and, finally, the rodlike textures are destroyed at 185°C. This process is in good agreement with the decrease in birefringence with temperatures beyond 160°C shown in Figure 11.

The scattering from the 25/75 blend film with  $\lambda=40$  at 20°C shows an X-type pattern whose lobes are slightly extended in the horizontal direction, characterizing the scattering from rodlike textures oriented in the stretching direction. The pattern becomes indistinct with increasing temperature but it preserves X-type even at 190°C. This indicates that the rodlike textures remain at 190°C. The aggregation of molecular chains with highly orientational degree seems to behave enough like rigid bodies to prevent large orientational fluctuation even at 190°C. This concept supports the birefringence data of the 25/75 blend film with  $\lambda=40$  in Figure 12.

Finally, we shall discuss whether the complex dynamic moduli in Figures 3–7 can be analysed on the basis of a composite law. Let the composite structural unit be as Figure 14, in which polyethylene layers lie adjacent to polypropylene layers with the interfaces perpendicular to the  $X_3$  and  $X_1$  axes, so that the strains of the two phases at the boundaries are identical. In this model system, the  $X_3$  and  $X_1$  axes may be taken along the stretching and thickness (or transverse) directions. The volume crystallinity  $X_0$  is represented as the product  $\delta\mu$  of the fractional lengths  $\delta$  and  $\mu$  along the  $X_3$  and  $X_1$  axes.

According to Maeda *et al.*<sup>22</sup>, the complex dynamic modulus  $E^*$  in the  $X_3$  direction is given by

$$E^* = \frac{\mu}{S_{33}^{I*}} + \frac{1-\mu}{S_{33}^{PP*}} + \frac{\left(\frac{S_{13}^{I*}}{S_{33}^{I*}} + \nu_{31}^{PP}\right)^2}{\frac{S_{33}^{PP*}}{1-\mu} \{1 - (\nu_{31}^{PP})^2\} + \frac{S_{33}^{I*}}{\mu} \left\{1 - \frac{(S_{13}^{I*})^2}{S_{11}^{I*} S_{33}^{I*}}\right\}} \quad (1)$$

where, for example,

$$\frac{1}{S_{33}^{I*}} = \frac{\delta}{S_{33}^{PE*}} + \frac{1-\delta}{S_{33}^{PP*}} + \frac{(-v_{13}^{PE} + v_{31}^{PP})^2}{\frac{S_{33}^{PP*}}{1-\delta} \{1 - (v_{31}^{PP})^2\} + \frac{S_{33}^{PE*}}{\delta} \{1 - (v_{31}^{PE})^2\}} \quad (2)$$

Similarly,  $S_{11}^{I*}$  and  $S_{13}^{I*}$  can be obtained from boundary conditions, although they are not represented in this paper.  $S_{ij}^{PE}$  and  $S_{ij}^{PP}$  denote the complex elastic compliances of polyethylene and polypropylene, respectively, and  $v_{ij}^{PE}$  and  $v_{ij}^{PP}$  are Poisson's ratios of polyethylene and polypropylene, respectively. In equation (1), we assume

$$\begin{aligned} S_{13}^{PE*} &= -v_{31}^{PE} S_{33}^{PE*} \\ S_{13}^{PP*} &= -v_{31}^{PP} S_{33}^{PP*} \end{aligned} \quad (3)$$

where  $S_{33}^{PE*}$  and  $S_{33}^{PP*}$  are related to the storage and loss moduli of polyethylene and polypropylene homopolymers as follows:

$$\begin{aligned} S_{33}^{PE*} &= \frac{1}{E'_{PE} + iE''_{PE}} \\ S_{33}^{PP*} &= \frac{1}{E'_{PP} + iE''_{PP}} \end{aligned} \quad (4)$$

Returning to Figures 3–7, the solid curves exhibit the calculated results for storage and loss moduli. They are in poor agreement with the experimental results except for the undrawn films in Figure 3. This disagreement probably arises from the assumption that the temperature dependences of the complex dynamic moduli of polyethylene and polypropylene phases within the blend films are equal to those within the individual homopolymers at each draw ratio. In fact, as can be seen in Figures 8 and 9, the orientation factors of the *c*-axes of polyethylene and polypropylene within the blend films are different from those within their individual homopolymers at each draw ratio and, especially at  $\lambda=20$ , the orientation factors are strongly affected by PE/PP composition, becoming lower with increasing polyethylene content. To obtain a better fit between experimental and calculated results, the PE/PP composition dependence on molecular orientation must be taken into account in further studies.

## SUMMARY AND CONCLUSIONS

Polyethylene-polypropylene blend films were prepared by gelation/crystallization from semidilute solutions by using ultrahigh molecular weight polyethylene ( $M_v = 6 \times 10^6$ ) and polypropylene ( $M_v = 4.4 \times 10^6$ ). The PE/PP compositions chosen were 75/25, 50/50 and 25/75. The mechanical properties of the blend gel films depended upon PE/PP composition, since the orientational degrees of the *c*-axes of polyethylene and polypropylene within the blend films are different from those of their individual

homopolymers. For the undrawn films, the storage modulus increases with increasing polyethylene content and the results calculated on the basis of a simple composite model are in good agreement with the experimental results. In contrast, Young's modulus (and the storage modulus) for the films with  $\lambda=20$  decreases with increasing polyethylene content. With further elongation beyond  $\lambda=40$ , Young's modulus (or the storage modulus) increases with increasing polyethylene content.

The complex dynamic moduli of the blend films with draw ratio beyond  $\lambda=20$  are in poor agreement with the results calculated on the basis of the model system. This disagreement is due to the fact that the molecular orientations of the polyethylene and polypropylene phases within the blend films are not equal to those of the individual homopolymers. Under the fixed dimension in the stretching direction, the 25/75 blend film with  $\lambda=40$  preserves the rodlike textures even at 190°C higher than melting point of polypropylene by the superheating effect. The birefringence at 190°C was slightly higher than that at 20°C, indicating further arrangement of molecular chains due to active thermal mobility. This indicated that polyethylene chains are not free to allow orientational fluctuation and are extended in the melt state.

## REFERENCES

- Matsuo, M. and Sawatari, C. *Macromolecules* 1986, **19**, 2036
- Sawatari, C. and Matsuo, M. *Macromolecules* 1986, **19**, 2653
- Matsuo, M., Sawatari, C. and Nakano, T. *Polymer J.* 1986, **18**, 759
- Sawatari, C. and Matsuo, M. *Colloid Polym. Sci.* 1985, **263**, 783
- Sawatari, C., Shimogiri, S. and Matsuo, M. *Macromolecules* 1987, **20**, 1033
- Smith, P., Lemstra, P. J., Kalb, B. and Pennings, A. J. *Polym. Bull.* 1979, **1**, 733
- Smith, P. and Lemstra, P. J. *J. Mater. Sci.* 1980, **15**, 505
- Smith, P., Lemstra, P. J. and Booij, H. C. J. *J. Polym. Sci., Polym. Phys. Edn.* 1981, **19**, 877
- Matsuo, M., Hirota, K. and Kawai, H. *Macromolecules* 1978, **11**, 1000
- Fujita, K., Suehiro, S., Nomura, S. and Kawai, H. *Polymer J.* 1982, **14**, 545
- Nakayasu, H., Markovits, H. and Plazek, D. J. *Trans. Soc. Rheol.* 1961, **5**, 261
- Takayanagi, M. and Matsuo, M. *J. Macromol. Sci. Phys.* 1967, **B1**, 407
- Suehiro, S., Yamada, T., Inagaki, H., Kyu, T., Nomura, S. and Kawai, H. *J. Polym. Sci., Polym. Phys. Edn.* 1979, **17**, 763
- Kawai, H., Suehiro, S., Kyu, T. and Shimomura, A. *Polym. Eng. Rev.* 1983, **3**, 109
- Matsuo, M., Sawatari, C. and Ohhata, T. *Macromolecules* 1987, **21**, 1317
- Wilchinsky, Z. W. *J. Appl. Phys.* 1960, **31**, 1969
- Matsuo, M. and Manley, R. S. T. *Macromolecules* 1982, **15**, 985
- Tsvetkov, V. N. 'Newer Methods of Polymer Characterization', Interscience, New York, 1964, p. 563
- Bunn, C. W. and de Daubeny, R. *Trans. Faraday Soc.* 1954, **50**, 1173
- Matsuo, M., Inoue, K. and Abumiya, N. *Sen-i-Gakkaishi* 1984, **40**, 275
- Sawatari, C. and Matsuo, M. *Macromolecules* 1989, **22**, 2968
- Maeda, M., Hibi, S., Ito, F., Nomura, S., Kawaguchi, T. and Kawai, H. *J. Polym. Sci. A-2* 1970, **8**, 1303